Pure Appl. Chem., Vol. 76, No. 9, pp. 1769–1779, 2004.
© 2004 IUPAC

Stoichiometric and catalytic CO_2 reductions involving TiFe-containing intermetallic hydrides

Mark V. Tsodikov[1,‡], Vladimir Ya. Kugel[1], Fatima A. Yandieva[1], Vladimir P. Mordovin[2], Alexander E. Gekhman[3], and Ilya I. Moiseev[4]

[1]A. V. Topchiev Institute of Petrochemical Synthesis, Russian Academy of Sciences, 29 Leninsky Prospect, Moscow 119991, Russia; [2]A. A. Baikov Institute of Metallurgy and Material Sciences, Russian Academy of Sciences, 49 Leninsky Prospect, Moscow 119991, Russia; [3]N. S. Kurnakov Institute of General and Inorganic Chemistry, Russian Academy of Sciences, 31 Leninsky Prospect, Moscow 119991, Russia; [4]I. M. Gubkin Russian State University of Oil and Gas, 65 Leninsky Prospect, Moscow 119991, Russia

Abstract: Thermoprogrammed desorption of H_2 from $[TiFe_{0.95}Zr_{0.03}Mo_{0.02}]H_2$ showed two forms of absorbed hydrogen. The first one is evolved from the intermetallic hydride under heating up to 185 °C under Ar (loosely bound hydrogen, LBH). The second portion of H_2 (strongly bound hydrogen, SBH) remains in the intermetallic hydride up to 700–920 °C. SBH reacts with CO_2 to give CO rather selectively (80–99 %) at CO_2 conversion of 50–70 % at 350–430 °C and 10–12 atm. Dehydrogenation of cyclohexane coupled with CO_2 hydrogenation into CO predominantly proceeds efficiently in the presence of the intermetallic hydride $[TiFe_{0.95}Zr_{0.03}Mo_{0.02}]H_x$ (where $x \leq 0.1$) in a combination with industrial Pt/Al_2O_3 catalyst. Aliphatic primary alcohols undergo oxidation by CO_2 forming aldehydes in the presence of $[TiFe_{0.95}Zr_{0.03}Mo_{0.02}]H_{0.36}$. Conversion of the alcohols into alkanes with carbon skeleton counting at least doubled carbon number in comparison with parent alcohol was found to be catalyzed by the mixture of the last intermetallic hydride and Pt/Al_2O_3 catalyst.

INTRODUCTION

The world's reserves of fossil fuels (natural gas, oil, and coal) count 10^{13} t of carbon. The global amount of CO_2 and its derivatives on Earth, including the atmosphere and oceans, is at least 10 times larger counting 10^{14} t of carbon. Carbon dioxide is both an industrially renewable raw material and an atmospheric pollutant, one of the major contributors to the greenhouse effect.

Gas-works processing natural gas produce CO_2 as a final product. Many electric power stations produce exhaust gases concentrated in respect to carbon dioxide suitable for a chemical use. Utilization of carbon dioxide is both an important ecological problem and a challenging goal of C_1 chemistry [1].

In this paper, both stoichiometric and catalytic CO_2 reductions involving intermetallic hydrides of general composition $[TiFe_{0.95}Mo_{0.02}Zr_{0.03}]H_x$ where $2 \geq x \geq 0.1$ in a combination with industrial Pt/Al_2O_3 catalyst were studied.

---

*Plenary lecture presented at the XVII Mendeleev Congress on General and Applied Chemistry, Kazan, Tatarstan, Russia, 21–26 September 2003. Other presentations are published in this issue, pp. 1605–1798.

‡Corresponding author: E-mail: tsodikov@ips.ac.ru

In the presence of metal-containing catalysts, hydrogenation of CO_2 to give methanol, a number of gaseous C_1–C_4 hydrocarbons, and CO proceeds most readily [2–6]. Carbon dioxide also enters into reverse water gas shift reaction (RWGSR), giving rise to CO and light hydrocarbons, mainly methane [2–7]. More selective transformation of CO_2 into CO occurs in the presence of metal oxide and sulfide catalysts [7,8]. Thus, the selectivity of CO_2 reduction into CO reaches 97 % in the presence of preliminarily reduced iron/alumina catalyst. However, CO_2 conversion remains low [8,9]. Selective formation of CO was observed as well in CO_2 hydrogenation on a Pd–Ru membrane modified by a nickel coating [10]. In the presence of cobalt and iron filamentary crystals with special-purity quartz particles, direct transformation of CO_2 into ethylene and propylene was attained; the content of these products in the gas mixture was up to 10 % [11].

Among CO_2 reductions with dihydrogen, only methanation and methanol synthesis are allowed thermodynamically at standard conditions (see Table 1).

Table 1 Thermodynamics of reactions involving CO_2 (kj/mol) [12].

Reactions	ΔH^Θ	$-T\Delta S^\Theta$	ΔG^Θ
$H_{2(g)} + CO_{2(g)} \rightarrow CO_{(g)} + H_2O_{(g)}$	41.20	22.6	18.60
$H_{2(g)} + CO_{2(g)} \rightarrow CO_{(g)} + H_2O_{(I)}$	–2.80	22.8	20.00
$H_{2(g)} + CO_{2(g)} \rightarrow HCOOH_{(I)}$	–31.20	64.2	33.00
$2H_{2(g)} + CO_{2(g)} \rightarrow CH_2O_{(g)} + H_2O_{(I)}$	–9.00	55.0	44.00
$3H_{2(g)} + CO_{2(g)} \rightarrow CH_3OH_{(I)} + H_2O_{(I)}$	–131.30	122.1	–9.2
$4H_{2(g)} + CO_{2(g)} \rightarrow CH_{4(g)} + 2H_2O_{(I)}$	–252.90	122.1	–130.80
$CO_{2(g)} + CH_{4(g)} \rightarrow 2CO_{(g)} + 2H_{2(g)}$	191.8	–	288.0

EXPERIMENTAL

The intermetallic compounds $TiFe_{0.95}Zr_{0.03}Mo_{0.02}$ and TiFe were prepared by the consumable-electrode melting of starting components. Titanium sponge (TG 100), low-carbon steel (Russian State Standard 11036-75), zirconium iodide, and molybdenum metal were used as starting materials. To protect the TiFe alloy from contamination by impurities, the method of scull melting [13] was used in this study.

To evaluate apsorption capacity, the isotherms of hydrogen apsorption by the intermetallics were registered using a high-pressure manometric unit made of stainless steel. The alloys were crushed to particle size of 0.5–1.0 mm. A reaction vessel of 200-ml volume was loaded with 50 ± 0.5 g of an alloy pulver and evacuated to a pressure of 10^{-3} torr. Thereafter, the intermetallic compound was activated by treatment with hydrogen at 70–80 atm and 20 °C. The material was held under these conditions until the reactor temperature began to rise; the heating was indicative of the chemical dissolution of hydrogen in the alloy. The time interval from the beginning of the alloy treatment with hydrogen to the beginning of reactor heating was designated as the activation period. After activating a sample, the reactor was carefully pumped out and then filled with hydrogen to a certain pressure at 20 °C. The amount of absorbed hydrogen was estimated from the difference between the initial and final pressure. The equilibrium hydrogen pressure corresponding to each experimental point of an absorption curve, registered using a high-precision reference pressure gauge after maintaining the system for no less than 10 h after of a constant H_2 pressure, is established. Approximately 1 mol of H_2 was absorbed per one intermetallic unit $TiFe_{0.95}Zr_{0.03}Mo_{0.02}$ corresponding to $[TiFe_{0.95}Zr_{0.03}Mo_{0.02}]H_2$ hydride formation.

The activation period for an undoped TiFe alloy exceeded 24 h, which is much longer than the analogous period for the doped intermetallide (~0.5 h).

The temperature-programmed desorption (TPD) of hydrogen from the $[TiFe_{0.95}Zr_{0.03}Mo_{0.02}]H_2$ hydride and catalytic experiments was studied by using a high-pressure flow-circulation set-up. A flow

of argon was circulated while temperature increases at a rate of 10 K/min at up to 920 °C. The amount of desorbed hydrogen was determined by using an LKhM-80 chromatograph with a column (1.5 m × 4 mm) packed with an SKT carbon adsorbent at 60 °C and argon as the carrier gas and TPI detector.

The $TiFe_{0.95}Zr_{0.03}Mo_{0.02}$ intermetallic, an industrial platinum/alumina catalyst, and their mixture were used as catalysts for CO_2 hydrogenation. Prior to loading into the reactor, the intermetallic was crushed to ~2–3-mm pellets using a ball mill with corundum balls. The intermetallic and Pt/Al_2O_3 mixtures were prepared as a thoroughly mixed blend consisting of 2–3-mm pellets of the intermetallic and small cylinders of the industrial Pt/Al_2O_3 catalyst. The mixture of finely ground intermetallic compound (60 g) and Pt/Al_2O_3 catalyst (6.3 g) was loaded in the reactor and the resulting heterogeneous system was treated with hydrogen at 100 °C and 1 atm under H_2 flow for 10–14 h (activation). After activation, the system was cooled to 25–30 °C, and high-pressure (120–135 atm) H_2 was rapidly fed in the circulation mode. CO_2 hydrogenation was carried out within the interval of 350–430 °C and 10–12 atm. The reaction products were analyzed by gas chromatography in the online mode using an LKhM 80 MD chromatograph. The gas components were identified by adding reference compounds, their concentrations were calculated by the absolute method as described in [13].

RESULTS AND DISCUSSION

The solubility of H_2 in $TiFe_{0.95}Zr_{0.03}Mo_{0.02}$ is much higher than that in TiFe alloy at hydrogen pressure. A plateau at saturation pressure P(1) ≈ 12.5 atm is clearly defined in the absorption isotherm of TiFe (Fig. 1).

The initial area of H_2 absorption by the TiFe intermetallic was attributed to the formation of the so called α-phase, a solid solution of hydrogen in the intermetallic compound of the composition $[TiFe]H_x$, where $x \approx \leq 0.1$. [17] The plateau is attributed to a mixture of α and β phases with transition to the single-phase state of the β solution. The individual β phase was attributed to $x \approx 0.7$–0.8.

Additional dissolution of hydrogen in the β phase was observed above 20 atm H_2 pressure. The isotherm of H_2 absorption by the $TiFe_{0.95}Zr_{0.03}Mo_{0.02}$ exhibits a plateau corresponding to a saturation pressure of ~2 atm (Fig. 1) and a dramatic increase after this plateau. After the plateau region, the absorption curve exhibits a dramatically increased after this plateau.

Thus, the absorption data suggest that the interaction of H_2 with the $TiFe_{0.95}Zr_{0.03}Mo_{0.02}$ intermetallic is noticeably different from the interaction of hydrogen with the undoped TiFe alloy: a hydride phase corresponding to the intermetallic compound $TiFe_{0.95}Zr_{0.03}Mo_{0.02}$ was formed at a considerably lower pressure (~2 atm) than the α-phase in the case of $TiFeH_x$ (12.5 atm). Moreover, the formation of intermetallic $TiFe_{0.95}Zr_{0.03}Mo_{0.02}$ hydrides is characterized by a much shorter activation period (~0.5 h) than that for TiFe hydride (over 24 h).

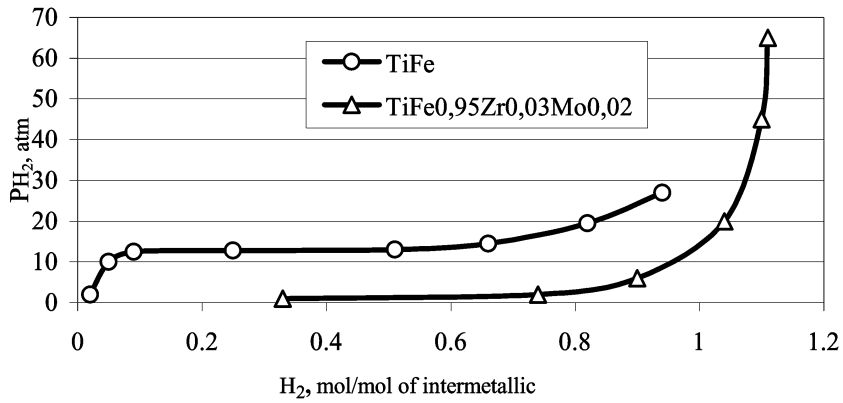

Fig. 1 Isotherms of hydrogen absorption by the TiFe and $TiFe_{0.95}Zr_{0.03}Mo_{0.02}$ intermetallic at 20 °C.

The $H_2/[TiFe_{0.95}Zr_{0.03}Mo_{0.02}]$ system

The experiments showed 1 mole of $TiFe_{0.95}Zr_{0.03}Mo_{0.02}$ to absorb 1 mole of H_2. The curve of the thermal desorption of adsorbed hydrogen from a sample with the stoichiometric composition $[TiFe_{0.95}Zr_{0.03}Mo_{0.02}]H_2$ in an argon atmosphere (Fig. 2) clearly exibit three regions. The first of them corresponds to the intense release of ~0.80–0.82 mol of H_2 per mole of the sample on heating this hydride from 70 to 185 °C. This portion of H_2 can be conventionally referred to as loosely bound hydrogen (LBH). Practically no H_2 was released while the temperature further increased. The next part of the hydrogen absorbed by the intermetallic (i.e., ~0.09 mol H_2 per mole of the intermetallic compound) was evolved in the interval 700–920 °C. Much higher temperatures are required for the thermal desorption of the remaining hydrogen (~0.09 mol/mol).

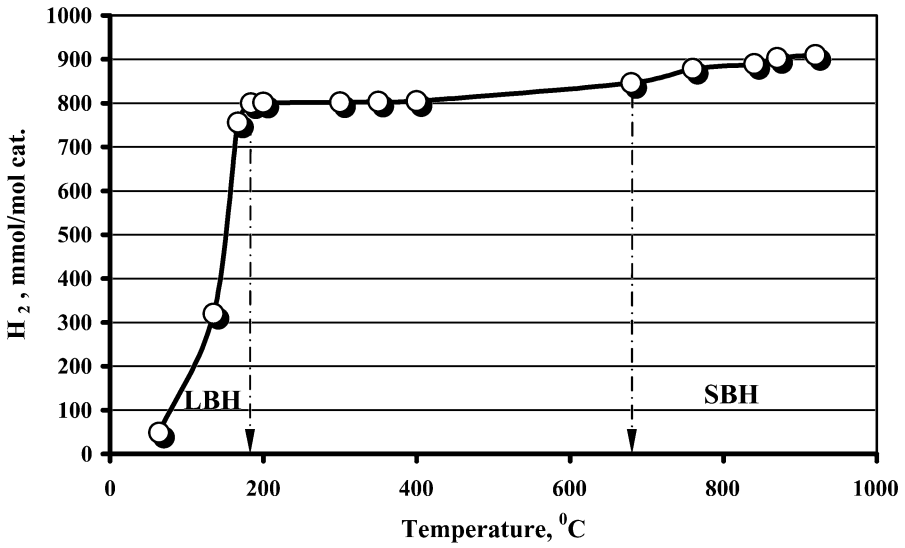

Fig. 2 H_2 desorption at linear programmed temperature increases from $[TiFe_{0.95}Zr_{0.03}Mo_{0.02}]H_2$ sample.

The intermetallic hydride $[TiFe_{0.95}Zr_{0.03}Mo_{0.02}]H_{0.36}$ formed after heating the hydride $[TiFe_{0.95}Zr_{0.03}Mo_{0.02}]H_2$ up to 700 °C contains so-called strongly bound hydrogen (SBH).

As a whole, thermodesorption of dihydrogen from $[TiFe_{0.95}Zr_{0.03}Mo_{0.02}]H_2$ could be presented by the Scheme 1:

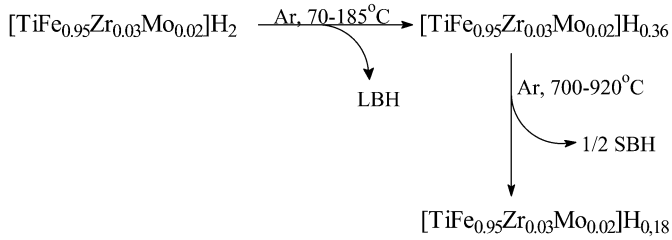

Scheme 1 Interconversions of intermetallic hydride $[TiFe_{0.95}Zr_{0.03}Mo_{0.02}]H_2$.

It is known that hydride phases obtained from hydrogen-accumulating intermetallic compounds are characterized by different strengths of hydrogen binding [16–18]. Actually, the $[TiFe_{0.95}Zr_{0.03}Mo_{0.02}]H_x$ intermetallic compound ($x \sim 2$) react with CO_2 to give CO and small amounts

of methane at 20 °C [14,15]. SBH-containing intermetallic is less reactive but more selective in CO_2 reduction. The selectivity of CO_2 hydrogenation depends on the way of hydrogen supply to the reaction volume.

Part of SBH can be removed from intermetallic hydride $[TiFe_{0.95}Zr_{0.03}Mo_{0.02}]H_{0.36}$ by treatment with CO_2 at 350–430 °C:

$$[TiFe_{0.95}Zr_{0.03}Mo_{0.02}]H_{0.36} + CO_2 \rightarrow CO + H_2O + [TiFe_{0.95}Zr_{0.03}Mo_{0.02}]H_f \text{ where } 0.18 \geq f \geq 0.1$$

After the repeated supply of high-pressure H_2 to the intermetallic $[TiFe_{0.95}Zr_{0.03}Mo_{0.02}]H_{0.36}$, absorption of ~0.6 mol H_2 takes place once again. Thus, after the repeated absorption, the total content of hydrogen in the intermetallic system approaches again the amount of H_2 initially absorbed by the fresh intermetallic $TiFe_{0.95}Zr_{0.03}Mo_{0.02}$.

The N_2 adsorption measurements showed that the initial intermetallic compound does not possess a developed surface, whereas after H_2 absorption and subsequent desorption, the specific surface area of the material is 0.06 ± 0.02 m^2g^{-1}. It can be noted that this is a fairly high value for a metallic surface.

An increase in the specific surface area of a hydrogen-accumulating system after absorption–desorption procedures has been described previously for nickel zirconium intermetallic (ZrNi) compounds [3].

Stoichiometric CO_2 reductions

The CO_2 reductions with intermetallic hydrides can be presented by Scheme 2:

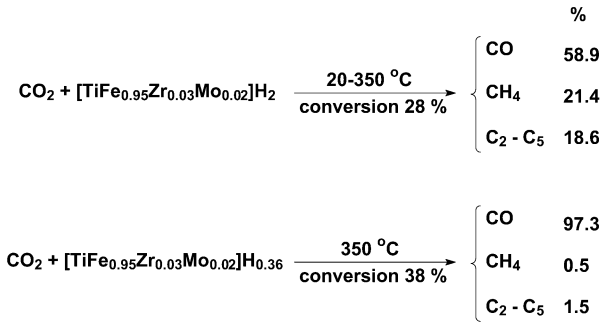

Scheme 2 O2 Reactions with intermetallic hydrides (10 atm, t = 4 h).

Hydrogenation of CO_2 with SBH ($[TiFe_{0.95}Zr_{0.03}Mo_{0.02}]H_{0.36}$) gives rise predominantly to CO at 350–430 °C. The yield of C_1–C_5 hydrocarbons is rather low. For instance, 60 % of carbon dioxide was converted into CO with a selectivity of 80 % during the first hour at 430 °C. Virtually 71 % conversion of CO_2 was observed in the second hour of CO_2 circulation, but the selectivity of CO formation decreased to 59 % and the yield of hydrocarbons increased. A much lower CO_2 conversion (22 %) with the selectivity of CO_2 reduction to CO being very high (98–100 %) was observed after replacement of the hydrogenation products by fresh CO_2. These data indicate that hydrocarbons might result from CO hydrogenation.

The selectivity of CO formation did not exceed 15–18 % at the conversion of CO_2 equal to 40 % in the reaction of H_2 and CO_2 mixture in the presence of Pt/Al_2O_3 catalyst (430 °C, 10 atm). The major reaction products were C_1–C_4 hydrocarbons, mainly methane (see Table 2).

Table 2 The selectivity of CO_2 hydrogenation. Influence of reagent nature (430 °C 10–12 atm.).

Reagent	$\tau_{45\ \%}$/h	W_0/mmol/g_{cat} h	Sco/%	Product CO	Composition/ CH_4	mol% C_2–C_5
$[TiFe_{0.95}Zr_{0.03}Mo_{0.02}]H_{0.36}$	0.25	3.3	85	85	8.5	6
$Pt/\gamma Al_2O_3$ (CO_2:H_2=1:1)	23	0.34	42	42	28	10
$[TiFe_{0.95}Zr_{0.03}Mo_{0.02}]H_{0.36}$ + $Pt/\gamma Al_2O_3$	0.25	3.7	99	99	0.1	0.5[a]

[a]+0.4 % – formaldehyde

In the presence of $[TiFe_{0.95}Zr_{0.03}Mo_{0.02}]H_{0.36}$ and Pt/Al_2O_3 mixture, the conversion of CO_2 reaches 58 % with the selectivity of CO formation being 98–100 % at 430 °C.

When intermetallic catalyst or its mixture with Pt/Al_2O_3 is used, the CO_2 conversion rapidly decreases during the experiment. However, after removal of the hydrogenation products by Ar circulation and subsequent replacement of Ar by fresh CO_2, the activity in CO_2 hydrogenation was restored until the SBH is exhausted.

Slow evolution of SBH into the gas phase of the reaction vessel was observed during CO_2 reduction. The H_2 accumulation causes decrease of CO selectivity due to more extensive hydrogenation of carbon oxides with hydrogen on the intermetallic surface as a secondary process.

The correlation between the selectivity of CO formation and SBH content in the reaction system suggests the participation of SBH in the reactions, giving rise to CO formation. Both the reduction of CO_2 to hydrocarbons and, possibly, carbon deposition on the surface of the heterogeneous system occurs at the cost of gas-phase H_2.

The amount of carbon deposed on the surface of intermetallic $[TiFe_{0.95}Zr_{0.03}Mo_{0.02}]H_{0.36}$ after 11 h reaction was found to be equal to 0.14 g and corresponded to the transformation of 0.012 mol of CO_2 into carbon. The total amount of converted CO_2 was 0.079 mol. Most part of CO_2 (84.8 %) was converted into CO and C_1–C_5 hydrocarbons, while 15.2 % was converted into carbon.

Apparently, the selective reduction of CO_2 to CO is a result of stoichiometric reaction between CO_2 and hydride atoms of SBH bound to the metal atoms of the intermetallic lattice, whereas hydrocarbon formation involves hydrogenation of CO with H_2 from the gas phase on the catalyst surface. Typical kinetic curves for the CO_2 transformation in the presence of intermetallic and Pt/Al_2O_3 mixture catalyst (Fig. 3) show that the rate of transformation of CO_2 decreases as carbon monoxide accumulates in the reaction vessel. The curve for CO accumulation has a maximum. A weakly pronounced induction period is typical for the plot of the hydrocarbon yield vs. the reaction time. All the data mentioned above and the increase of hydrocarbon yield while the CO content decreases is in agreement with the conclusion about the consecutive character of CO_2 hydrogenation: $CO_2 \rightarrow CO \rightarrow C_1$–$C_4$.

One of the major components of intermetallic catalyst is iron. The formation of stable iron carbonyl complexes can be expected to prevent chemisorptions of CO_2 on the active sites of $[TiFe_{0.95}Zr_{0.03}Mo_{0.02}]H_x$. The decrease of the SBH hydride atoms diffusion rate through the lattice of intermetallic $[TiFe_{0.95}Zr_{0.03}Mo_{0.02}]H_x$ toward the surface might be an additional factor leading to the decrease in CO_2 conversion in the stoichiometric reaction.

Note that different activity in hydrogenations catalyzed by nickel metal was ascribed to a difference in the reactivity of surface-located H atoms originated from bulk metal and gas-phase dihydrogen [19].

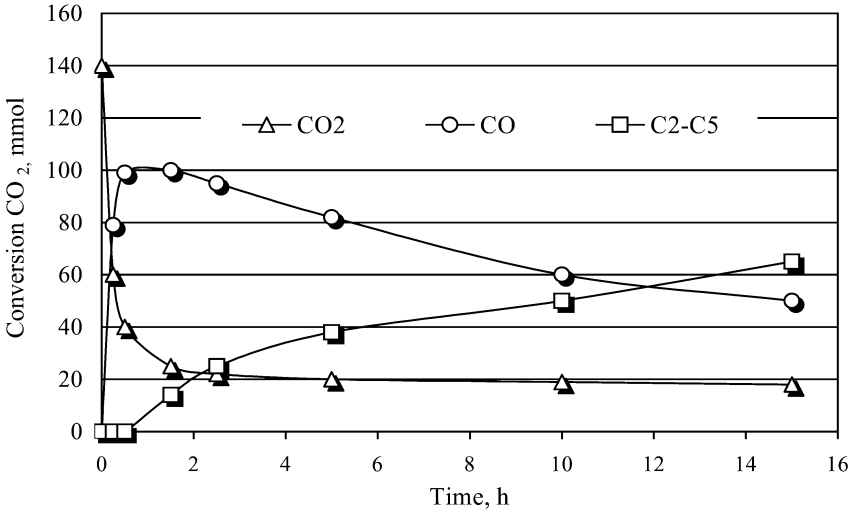

Fig. 3 Typical kinetics of CO_2 hydrogenation.

The initial rate of CO_2 reduction with H_2 in the presence of the platinum/alumina catalyst is an order of magnitude lower than the initial rate of stoichiometric reactions of CO_2 with $[TiFe_{0.95}Zr_{0.03}Mo_{0.02}]H_x$ or mixture of $[TiFe_{0.95}Zr_{0.03}Mo_{0.02}]H_x$ and Pt/Al_2O_3 (see Table 3).

Table 3 CO_2 reduction coupled with cyclohexane dehydrogenation at 430 °C and 10 atm; $V_{C6H12} = 0.1\ h^{-1}$.

Catalytic system	c-C_6H_{12} conversion %	S_{C6H6}, %	S_{CO}, %	$W_0^{CO_2}$ mmol/mol cat h
$[TiFe_{0.95}Zr_{0.03}Mo_{0.02}]H_f$ $f << 0{,}36$	02.5	68.8	90	25
$[TiFe_{0.95}Zr_{0.03}Mo_{0.02}]H_f$ $+Pt/\gamma Al_2O_3$	49	92.3	85	50
$Pt/\gamma Al_2O_3$	97	85.8	15	5

Catalytic reductions

CO_2 reductions with hydrocarbons are thermodynamically restricted under standard conditions. The reaction CO_2/CH_4 requires much higher temperature than CO_2/C_6H_{12} reaction owing to entropy factor. Dehydrogenation of cyclohexane catalyzed by nickel zirconium intermetallic (ZrNi) compound in a composition with the platinum/alumina catalyst gives rise to benzene in a yield substantially exceeding that one attained in the presence of Pt/Al_2O_3 catalyst [23].

Cyclohexane dehydrogenation coupled with the CO_2 reduction was studied by using catalyst $[TiFe_{0.95}Zr_{0.03}Mo_{0.02}]H_f$ and its mixture with Pt/Al_2O_3. The SBH-containing intermetallic $[TiFe_{0.95}Zr_{0.03}Mo_{0.02}]H_{0.36}$ has been treated with CO_2 at 430 °C to remove most part of SBH and get $[TiFe_{0.95}Zr_{0.03}Mo_{0.02}]H_f$.

Both components of the mixture by itself are also active. The activity of the pure $[TiFe_{0.95}Zr_{0.03}Mo_{0.02}]H_f$ catalyst is much lower than that of the industrial Pt/Al_2O_3 catalyst or the mixture of the intermetallic with the latter. The selectivity of benzene production is falling down in the row:

$$[TiFe_{0.95}Zr_{0.03}Mo_{0.02}]H_f + Pt/Al_2O_3 \geq Pt/Al_2O_3 > [TiFe_{0.95}Zr_{0.03}Mo_{0.02}]H_f.$$

During cyclohexane dehydrogenation, the concentration of molecular hydrogen in the reaction volume markedly increases. This is accompanied by a substantial increase in the rate of CO_2 hydrogenation (see eq. 1).

$$\begin{array}{c} c\text{-}C_6H_{12} \rightarrow C_6H_6 + 3H_2 \\ 3CO_2 + 3H_2 \rightarrow 3\ CO + 3H_2O \\ \hline c\text{-}C_6H_{12} + 3CO_2 \rightarrow C_6H_6 + 3H_2O + 3CO \end{array} \quad (1)$$

In parallel to the coupled reaction (eq. 1), uncoupled dehydrogenation of cyclohexane proceeds and a number of side reactions take place. For instance, an increase in the concentration of molecular hydrogen in the reaction vessel decreases the selectivity of CO formation due to extensive hydrogenation of CO_2 by molecular hydrogen into hydrocarbons as depicted by Fig. 4.

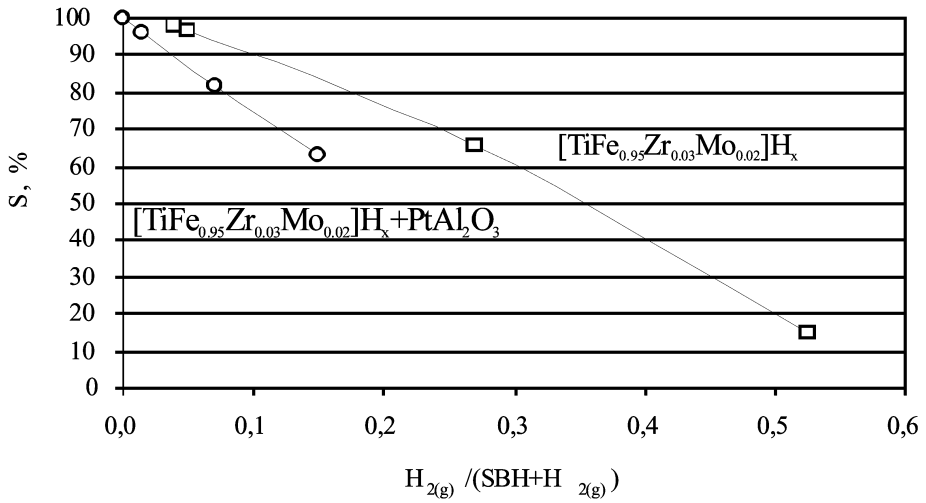

Fig. 4 Selectivity of CO_2 into CO conversion as a function of H_2 content in reaction vessel atmosphere (T = 430 °C, P = 10 atm).

Even after termination of the cyclohexane supply to the reaction zone, prolonged circulation of the gaseous products over catalysts $[TiFe_{0.95}Zr_{0.03}Mo_{0.02}]H_f$ or the mixture of $[TiFe_{0.95}Zr_{0.03}Mo_{0.02}]H_f$ with Pt/Al_2O_3 results in the formation of CO and hydrocarbons from CO_2. However, some amount of hydrogen formed via dehydrogenation of cyclohexane is obviously absorbed by the intermetallic compound forming SBH. It looks like the vacancies for SBH in the $[TiFe_{0.95}Zr_{0.03}Mo_{0.02}]H_f$ intermetallic hydride are used to be filled with absorbed hydrogen atoms. As a consequence of SBH's formation, the selectivity of CO formation reaches again 99–100 % at the carbon dioxide conversion equal to ~20 % after the replacement of hydrogenation products by fresh CO_2.

Cyclohexane hydrogenolysis reactions take place to a minor extent in parallel with the reactions mentioned above.

Aliphatic primary and secondary alcohol could be expected to react with CO_2 serving as hydrogen donors. For instance, ethanol, propanol-2, 2-methylpropanol-1, 3-methylpropanol-1, and 3-methylbutanol-1 have been proved to be involved into reducing CO_2 at 350 °C and 50 atm in the presence of $[TiFe_{0.95}Zr_{0.03}Mo_{0.02}]H_{0.36}$ and Pt/Al_2O_3. Aldehydes are expected products of alcohol oxidation by CO_2 (see eq. 2).

$$CO_2 + RCH_2OH \rightarrow CO + H_2O + RCHO \quad (2)$$

Ethers and esters were found among the products of the reaction besides CO. However, two important results should be stressed in the context of the reaction under consideration. The first one is a rather high yield of diisopenthylformal in the reaction of CO_2 with 3-methylbutanol-1 (see eq. 3):

$$2(CH_3)_2\text{-}CH\text{-}CH_2CH_2OH + CO_2 + 2H_2 \rightarrow [(CH_3)_2\text{-}CH\text{-}CH_2CH_2O]_2CH_2 + 2H_2O \quad (3)$$

Another point is unexpectedly high yield of hydrocarbons formed from an alcohol under the condition of CO_2/alcohol reduction. A detailed study showed that hydrocarbons are formed in a new channel of alcohol transformation, in which two or more alcohol molecules react with hydrogen splitting off water molecules and giving rise to an alkane molecule with linear or branched carbon skeleton [25].

For instance, most part of 3-methylbutanol was converted into 2,7-dimethyloctane (see eq. 4).

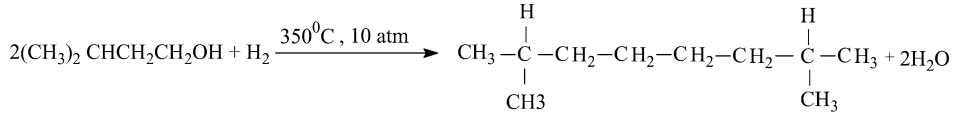

(4)

The reaction will be discussed in details elsewhere.

CONCLUSION

The data discussed above showed the intermetallic compounds $[TiFe_{0.95}Zr_{0.03}Mo_{0.02}]H_x$ to contain two types of absorbed hydrogen, one being strongly bound and the other being weakly bound to the intermetallic lattice. The reactivities of these forms of hydrogen toward CO_2 hydrogenation are different. The selective reduction of CO_2 into CO is attained only when SBH is involved in the process. The involvement of hydrogen from gas-phase gives rise predominantly to the reduction of CO to hydrocarbons.

Typically, absorption of H_2 by hydrogen-accumulating systems like TiFe is accompanied by the formation of a boundary layer of interstitial solid solutions and hydride phases characterized by a constant composition [16]. It has been noted, however, that absorption of H_2 by TiFe intermetallic compound starts only after the iron metallic phase is formed [16]. In this context, the weak catalytic activity of the binary system (TiFe) toward the dissociation of hydrogen activation could be rationalized.

Modification of the intermetallic compound with a minor amount of Zr and Mo makes it possible to accelerate markedly the process of H_2 absorption with retention of the cubic crystal structure and relatively high absorption capacity [17,18,24].

The Mössbauer spectroscopy and SANES data showed that inclusion of hydrogen into the TiFe structure brings about a substantial decrease in the electron's occupancy of the valence level of iron atoms, suggesting partial transfer of the electron density to the hydrogen atoms captured by the lattice [16]. In contrast, both XAFS and Mössbauer data suggest that H atoms of intermetallic hydride $[TiFe_{0.95}Zr_{0.03}Mo_{0.02}]H_{0.36}$ are bound to Ti, Zr, and Mo atoms, but not to Fe [24]. Note that all three transition elements bound to H atoms reveal enhanced affinity toward oxygen atom.

Evidently, the high rate of CO_2 reduction with SBH and the enhanced selectivity of CO formation are due to chemisorption of CO_2 on the sites containing hydride hydrogen. The subsequent steps may involve destruction of the surface intermediate formyl groups to give CO and water, analogously to the mechanistic schemes postulated in homogeneous catalysis [1,26].

After hydrogen attached to the intermetallic surface is completely consumed for the reduction of CO_2, a vacancy will appear in the coordination sphere of the hydride-forming metal atom. Hydrogen atom migration from the bulk intermetallic toward those vacancies of the surface can contribute to the process.

This can account for the fact that during the reduction of CO_2, virtually all SBH is involved in the reaction with CO_2 in 350–400 °C interval.

The decrease in the rate of CO_2 reduction in the RWGSR, which takes place on the surface of nickel catalysts, is due to the strong adsorption of CO, which blocks the active sites [2,10]. The accumulation of CO on the surface of the system might result in the formation of stable iron carbonyl complexes, which hamper the access of CO_2 to the active sites. Treatment of the surface with Ar or fresh CO_2 restores the ability of $[TiFe_{0.95}Zr_{0.03}Mo_{0.02}]H_x$ to reduce CO_2.

The selectivity of CO_2 into CO conversion in the presence of the catalytic composition $[TiFe_{0.95}Zr_{0.03}Mo_{0.02}]H_x$ and Pt/Al_2O_3 at 350–430 °C is markedly higher than that in the presence of individual catalysts separately in the same temperature range. Among other reasons, this synergistic effect can be due to the transfer of hydride hydrogen originated on the surface of the intermetallic compound to the surface of the platinum/alumina catalyst by the spillover mechanism and its participation in the reduction of CO_2. Phase transfer of hydrogen is presumably favored by a strong contact between the pellets of the aluminoplatinum catalyst and highly dispersed intermetallic pulver arising as a result of the embrittlement of $[TiFe_{0.95}Zr_{0.03}Mo_{0.02}]H_x$. In the presence of the mixed catalyst, the absorption of H_2 starts at a lower temperature than in the presence of the individual intermetallic compound $[TiFe_{0.95}Zr_{0.03}Mo_{0.02}]H_x$. This fact is in agreement with the possible role of phase transfer of H_2 as well.

The phase transfer of H_2 is well known for hydrogenation reactions over mixed catalytic compositions [27]. In particular, a mixture consisting of the nickel zirconium intermetallic compound and the platinum/alumina catalyst [23,27] has revealed higher activity in hydrocarbon dehydrogenation than the individual components of the mixture. One of the most popular views on the spillover mechanism implies heterophase interaction of heterogeneous systems, resulting in tight contact of the surface layers of the pellets of different catalysts [28,29].

The components of the $[TiFe_{0.95}Zr_{0.03}Mo_{0.02}]H_x$ and Pt/Al_2O_3 mixture perform different functions of the catalytic system in CO_2 hydrogenation coupled with cyclohexane dehydrogenation. The first stage of this process gives molecular hydrogen in a relatively high concentration upon dehydrogenation of cyclohexane, which is catalyzed efficiently by Pt/Al_2O_3 catalyst, and, as a consequence, extensive hydrogenation of CO_2 to CO and light C_1–C_5 hydrocarbons takes place. However, some amount of H atoms abstracted from cyclohexane is absorbed by the intermetallic compound, forming SBH. This H-form is consumed almost entirely for CO_2 hydrogenation into carbon monoxide.

Primary alcohols have been proved to serve as hydrogen donors reducing CO_2 similarly to cyclohexane action. Under the reaction, a new catalytic reaction was observed. Intermetallic hydride containing SBH $[TiFe_{0.95}Zr_{0.03}Mo_{0.02}]H_{0.36}$ was shown to be a catalyst of reductive alcohol dehydration giving rise to alkanes of which the carbon skeleton counts more carbon atoms than the parent alcohol molecule. The dominant products of this reaction are alkanes and isoalkanes, the molecules of which contain at least doubled number of carbon atoms.

REFERENCES

1. A. Behr. In *Catalysis in C_1 Chemistry*, W. Keim (Ed.), pp. 150–197, D. Reidel Publishing, Dordrecht (1983).
2. R. P. A. Sneeden. *J. Mol. Catal*. **17**, 349 (1982).
3. V. V. Lunin and O. V. Kryukov. In *Catalysis. Fundamental and Applied Studies*, O. A. Petrich and V. V. Lunin (Eds.), pp. 86–98, MGU, Moscow (1987) (in Russian).
4. P. Braunstein, D. Matt, D. Mobel. *Chem. Rev.* **88**, 747 (1988).
5. P. G. Jessop, T. Ikariga, R. Noyori. *Chem. Rev.* **95**, 259 (1995).
6. O. V. Krylov and A. Kh. Mamedov. *Russ. Chem. Rev.* **64**, 877 (1995) (Engl. Transl.).
7. H. Ando, Y. Matsumura, Y. Souma. *J. Mol. Catal. A: Chem.* **154**, 23 (2000).
8. M. Pijolat, V. Perrichon, M. Primet, P. Bussiere. *J. Mol. Catal.* **17**, 367 (1982).
9. T. Osaki, H. Toada, T. Horiuchi, H. Yamakita. *React. Kinet. Catal. Lett.* **51**, 39 (1993).

10. V. M. Gryaznov, S. G. Gulгyanova, Yu. M. Serov, V. D. Yagodovskii. *J. Phys. Chem.* **55**, 1306 (1981) (Engl. Transl.).
11. V. M. Gryaznov, Yu. M. Serov, N. B. Polyanskii. *Dokl. Akad. Nauk.* **359**, 647 (1998). [*Dokl. Chem.*, 1998 (Engl. Transl.)].
12. D. R. Stull, E. F. Westrum, G. C. Sinke. *The Chemical Thermodynamics of Organic Compounds*, John Wiley, New York (1969).
13. M. V. Tsodicov, V. Ya. Kugelг, E. V. Slivinskii, F. A. Yandieva, V. P. Mordovin, I. I. Moiseev. *Russ. Chem. Bull.* **50** (7), 1201 (2001).
14. M. V. Tsodikov, V. Ya. Kugelг, E. V. Slivinskii, V. P. Mordovin. *Russ. Chem. Bull.* **44**, 1983 (1995) (Engl. Transl.)
15. M. V. Tsodikov, V. Ya. Kugel, E. V. Slivinskii, V. G. Zaikin, V. P. Mordovin, G. Colon, M. C. Hidalgo, J. A. Navio. *Langmuir* **15**, 6601 (1999).
16. G. K. Shenoy, B. D. Dunlab, P. J. Viccaro, D. Niarehos. In *Mossbauer Spectroscopy and Its Chemical Application*, J. G. Sberens and G. K. Shenay (Eds.), pp. 501–510, Academic Press, New York (1981).
17. *Hydrogen in Metals, II Application-Oriented Properties,* G. Alefeld and J. Volkl (Eds.), *Topics and Applied Physics*, pp. 1–430, Springer-Verlag, Berlin (1978).
18. K. N. Semenenko, V. V. Burnashova, N. A. Yakovleva, E. A. Ganich. *Russ. Chem. Bull.* **47**, 209 (1998) (Engl. Transl.).
19. S. T. Seyer. *Acc. Chem. Res.* **34**, 737 (2001).
20. V. P. Mordovin, M. V. Tsodikov, V. Ya. Kugelr, L. A. Vytnova, E. V. Slivinskii, F. A. Yandieva. *Proceedings II Int. Conference on the Problems of Energy Storage and Ecology in Mechanical Engineering, Power Engineering, and Transport*, IMASh Russian Academy of Sciences, Moscow, 2001 (in Russian).
21. The Netherlands Pat. 7513159, 1977.
22. Yu. V. Levinskii. *State Diagrams of Metals with Gases*, Metallurgy, Moscow (1975) (in Russian).
23. O. V. Chetina, V. V. Lunin, G. V. Isagulyants. *Bull. Acad. Sci. USSR, Div. Chem. Sci.* **37**, 2168 (1988) (Engl. Transl.).
24. D. I. Kochubey, V. V. Kriventsov, Yu. V. Maksimov, M. V. Tsodikov, F. A. Yandieva, V. P. Mordovin, J. A. Navio, I. I. Moiseev. *Kinet. Katal*. **44** (2), 165 (2003).
25. M. V. Tsodikov, V. V. Kugel, F. A. Yandieva, I. I. Moiseev. *Kinet. Katal*. **45** (6), 1–13 (2004). The reaction will be discussed in details elsewhere.
26. C. H. Cheng, D. E. Mendriksen, R. Eisenberg. *J. Am. Chem. Soc.* **99**, 2791 (1977).
27. W. C. Conner, G. M. Pajonk, S. J. Teichner. *Spillover of Sorbed Species, Adv. Catalysis* **34**, 1 (1984).
28. S. J. Tauster, S. C. Fung, R. L. Garten. *J. Am. Chem. Soc.* **100**, 170 (1978).
29. K. Fujimoto and S. Toyoshi. In *Proc. 7th Int. Congr. Catal.* 235 (1981).